Hungarian Academy of Sciences
Research Centre for Natural Sciences

Yearbook

2013

Institute of Technical Physics and Materials Science

http://www.ttk.mta.hu/
http://www.mfa.kfki.hu/

Microtechnology Department

Head: Gábor BATTISTIG, Ph.D., senior research fellow

Research Staff

- Zsófia BAJI, Ph.D.
- István BÁRSONY, corr.memb. of HAS
- Gábor BATTISTIG, Ph.D.
- László DÓZSA, Ph.D.
- Csaba DÜCSŐ, Ph.D.
- Zoltán FEKETE, Ph.D.
- Péter FÖLDESY, Ph.D.
- Péter FÜRJES, Ph.D.
- Zoltán HAJNAL, Ph.D.
- Nguyen Quoc KHÁNH, Ph.D.
- Zoltán LÁBADI, Ph.D.
- István LUKÁCSI, Ph.D.
- György MOLNÁR, Ph.D.
- Ákos NEMCSICS, D.Sc. (part time)
- Andrea Edit PAP, Ph.D. (part time)
- Anita PONGRÁCZ, Ph.D. (on leave)
- Vilmos RAKOVICS, Ph.D.
- Attila Lajos TÓTH, Ph.D.
- Erika TUNYOGI
- János VOLK, Ph.D.
- Zsolt ZOLNAI, Ph.D.

Technical Staff

- János FERENCZ (engineer)
- Levente ILLÉS (engineer)
- Csaba LÁZÁR (engineer)
- István RÉTI (engineer)
- Róbert HODOVÁN (engineer)
- András LÖRINCZ (engineer)
- Katalin VERESNÉ VÖRÖS (engineer)
- György ALTMANN (technician)
- Gabriella BIRÓ (technician)
- Sándor CSARNAI (technician)
- Tibor CSARNAI (technician)
- Magda ERŐS (technician)
- Károlyné PAJER (technician)
- Csilla ARIAS-SOTONÉ FARAGÓ (technician)
- Attila NAGY (technician)
- Magda VARGA (technician)

Ph.D. students

- Zsófia BÉRCZES
- Zoltán SZABÓ
- Ferenc BÍRÓ
- Máté TAKÁCS
- Róbert ERDÉLYI
- Gergely MÁRTON
- Tamás KÁRPÁTI

Diploma workers

- Kristóf PÉTERFI, B.Sc.
- Éva JELINEK, B.Sc.
- Hunor MENYHÁRT, B.Sc.
- Gergő János MIKULA, B.Sc.
- János RADÓ, B.Sc.
- Ágoston HORVÁTH, B.Sc.
- Kristóf KUBINA, M.Sc.
- Ádám LUTZ, M.Sc.
- Tamás PARDY, M.Sc.
- Ferenc TOLNER, M.Sc.
- Eszter TÓTH, M.Sc.

The main task of the Microtechnology Department is the research and development of physical, chemical/biochemical sensors and integrated systems:

- **MEMS** and MEMS related **technologies**, with special emphasis on CMOS compatibility.
- Development of novel microfluidic systems, their application in new fields of biochemistry, **BioMEMS**.
- **Sensor development** with special emphasis on micropellistor-type gas sensors, 3D force sensors, thermal sensors, gas flow sensors, etc.
- Development of Si and polymer based sensors for biomedical applications with special emphasis on **NeuroMEMS**.
- Development of semiconductor nanodevices, synthesis and charactirization of quasi-one-dimensional semiconducting nanostrucrures, their integratation into functional sensor, optoelectronic and photovoltaic devices - **NEMS**.

Fundamental research on:

- sensing principles;
- novel materials and nanostructures;
- novel 3D fabrication techniques;
- ion-solid interaction for supporting MEMS development.

Device and structural characterization methods widely used in our projects:

- Electrical characterization;
- Thermo-mechanical characterization;
- Scanning Microprobes;
- Ion beam analysis methods;
- SEM, TEM, EDX;
- Spectroscopic Ellipsometry.

The Microtechnology Department of MFA runs two 300 + 160 m^2 clean labs, respectively (Class 100-10000) comprising a complete Si-CMOS processing line and a mask shop, unique in Hungary. The facility is capable on 3" and 4" Si and glass wafers of manufacturing layers, patterned structures and devices with 1µm resolution.

Main processes in the Microtechnology lab (available also for our partners and customers):

- High temperature annealing, diffusion and oxidation;
- Rapid Thermal Treatment;
- Low Pressure Chemical Vapor Deposition of poly-Si, SiO2 and Si3N4 layers;
- Low Temperature Chemical Vapor Deposition;
- Ion implantation;
- Physical Vapor Deposition – Electron beam evaporation, DC and RF Sputtering;
- Atomic Layer Deposition;
- Reactive Ion Etching, Deep Reactive Ion Etching;

- Photolithography with back-side alignment and Nanoimprinting;
- E-beam lithography;
- Nanopatterning, deposition and etching by Focussed Ion-Beam;
- Wafer Bonding;
- Wet chemical treatments;
- Electro-chemical porous Silicon formation;
- Molecular Beam Epitaxy of III-V compound semiconductors;
- Mask design, laser pattern generator;
- Polymer (PDMS, SU8, Polyimide) structuring by photolithography and micromoulding techniques,
- Chip dicing, packaging especially for sensor applications;
- Materials and structural characterizations, Stylus Profiler, Electrochemical Impedance Spectroscopy, SEM, FIB, EDX, Atomic Force Microscopy;
- Electrical and functional characterization.

For detailed information please visit us at our web-site (http://www.mems.hu/) or contact us: dragon@mfa.ttk.hu

MEMS

Activity leader: Cs. Dücső
Group members: Zs. Baji, I. Bársony, G. Battistig, L. Dózsa, P. Földesy, P. Fürjes, Z. Hajnal, Z. Lábadi, G. Molnár, A. E. Pap, V. Rakovics, A. L. Tóth, E. Tunyogi, Zs. Zolnai, F. Biró, T. Kárpáti, and M. Takács

Activities are supported by
- OTKA K109674 - Graphen based terahertz modulators (2013-2017)
- OTKA K91154 - Environmentally friendly semiconductors: iron silicide nanostructures (2010-2013)
- OTKA CNK77564 - Terahertz sensing for THz imaging (2010-2013)
- KMR-12-1-2012-0107 – Sensor for continuous monitoring of carbonhydrides dissolved in underground water (2012-2015)
- KMR_12-1-2012-0031 – Development of an embedded information system for the optimisation of energy-positive public lighting (2012-2014)

Development of physical and chemical sensors

This activity of the MEMS lab focused on the development of existing gas and force sensor chips and related characterization methods, targeting application in commercial sensor systems.

Gas sensors

Having successfully demonstrated the operation of micro-pellistor and conductivity (Taguchi-type) sensors, their long term properties in terms of thermo-mechanical stability and functionality were investigated. For marketable products it is required to achieve several years of operation time without loss of sensitivity.

Accelerated ageing tests revealed that degradation of the present catalyst results in a sensitivity drop of 10% within a few weeks, therefore substantial improvement of the catalyst is required to provide a stable sensor response. Although the slurry-like catalyst was traditionally widely used in commercial Pt coil based pellistors, this mixture proved to be non-compatible with the thin film based microsensor structure. Besides, the thermo-mechanical stability of the micro-hotplate could also be improved to meet life-time expectations.

Based on FEM calculations of alternative structures the micro-hotplate geometry and its vertical multilayer construction were further optimized. The aim was to achieve operational temperature above 500 °C with a power dissipation below 20 mW and to facilitate a minimum displacement of the membrane during temperature shocks. The most promising layer structures were realised and tested in pulsed mode heating cycles between room temperature and 500 °C. After the first few thousand stabilizing periodes, the best devices were able to withstand up to 8×10^5 cycles corresponding to ca. 5 years of operation time. Nevertheless, electromigration effect induced

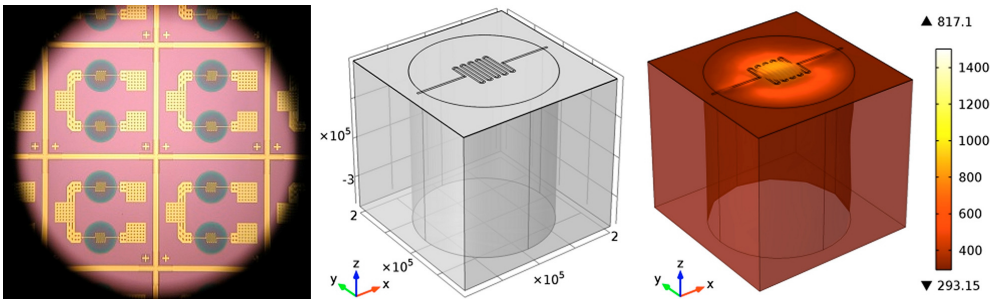

Figure 1. *Microscopic view of 4 sensor chips containing two microheaters (left), 3D FEM structure (centre), and thermal distribution at 12 mW heating power (right).*

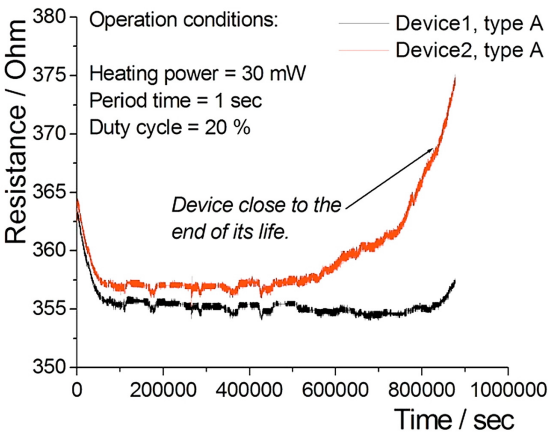

Figure 2. *Results of accelerated ageing tests.*

degradation of Pt filament must also be reduced, if continuous operation mode is selected. As the current density in the filament cannot be reduced without losing thermal isolation, we have started to investigate the effect of alternative adhesion layers on heater stability. Due to geometric and adhesion constraints application of conventional Pt based catalyst slurry droplets is far for being compatible with the thin film hotplate structure. Therefore, an appropriate thin film catalyst formation method must be elaborated. A laterally selective electrochemical process to provide a large surface was developed by formation of a thin (< 2 - 3 µm) porous alumina layer on the top of the hotplate. This layer is to support noble metal catalytic nano-particles to be deposited in a subsequent step. Beside sputtering and micro droplet methods for sensitizing the porous layer ALD (atomic layer deposition) is also considered. Optimization of pore size and porosity as well as testing alternative sensitizing techniques is the next step in process development. As a proof of concept, porous alumina catalyst support was covered with Pt by thermal decomposition of water dissolved $H_2[PtCl]_6$ droplets and devices were tested for hydrocarbon response.

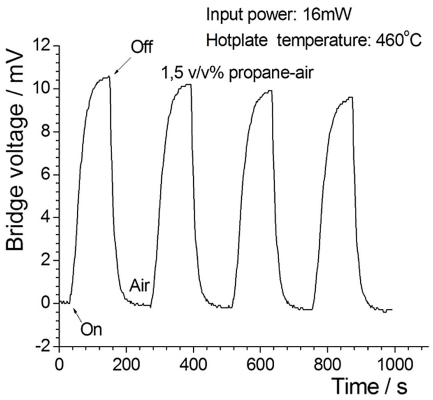

Figure 3. *Sensor response to 60% LEL of propane.*

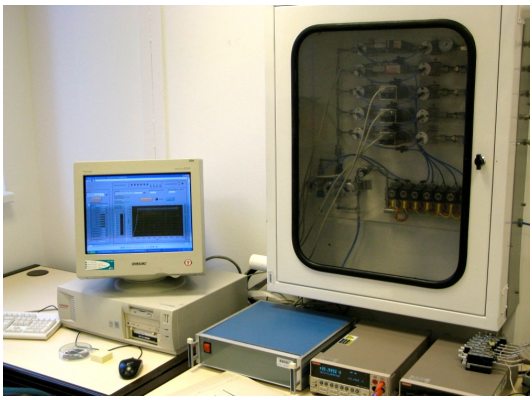

Figure 4. *Gas sensor test setup.*

For functional characterization of gas sensor chips a new test station was developed capable of introducing 3 different gases in synthetic air if needed. Besides measuring response time accurately, the gas concentration range can arbitrarily be set between ppm and 20v%.

3D micro-force sensor

A high yield, reliable processing technology for manufacturing three dimensional force sensors was demonstrated. The basis of the process is the adaptation of the existing technology for SOI (silicon on insulator) wafers to provide uniform membrane geometry over the whole wafer. Thereby, the deviation of chip characteristics could be harmonized with industrial process requirements. As by this technique the size of a single element force sensor can be reduced to ca. 1.5 × 1.5 mm^2, we hope to extend the application area of the device to biomedical/surgery field as well.

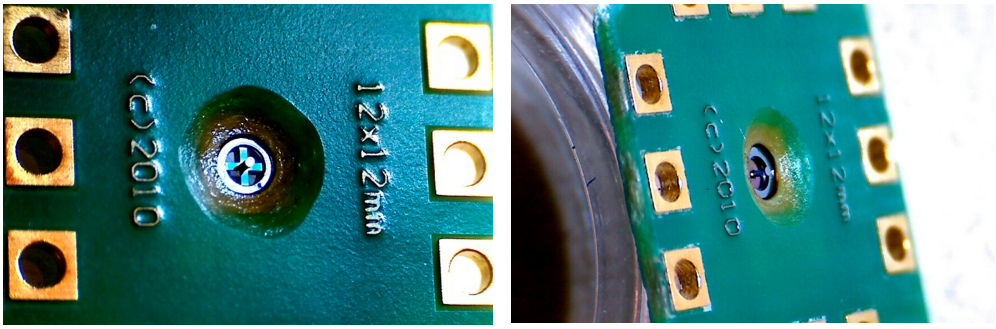

Figure 5. *3D micro force measuring chips with perforated (left) and full membranes (right). Both versions are fabricated in SOI wafers and assembled in a PC board for testing. Size of the sensing structure: 1 mm diameter.*

For individual testing and quick feedback of characteristics an accurate 3D vectorial-force loading station was also constructed.

Figure 6. *Setup for testing 3D micro-force sensor chip by an accurate force-vector load. Close-up view of the chip and the needle of the calibration force sensor are seen on the monitor of the system control PC.*

Sensor chips of alternative membrane structures were processed and assembled for characterization.

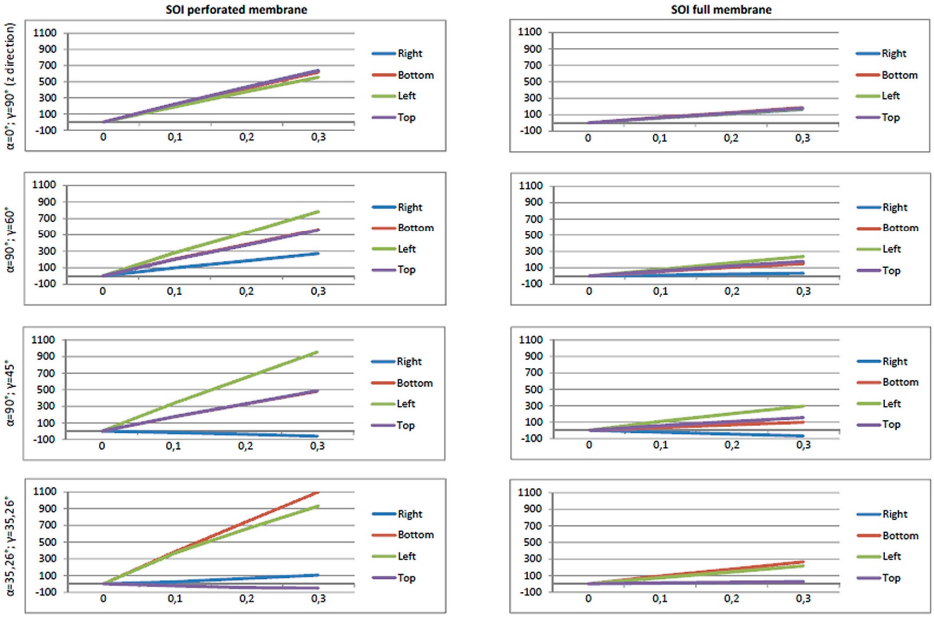

Figure 7. *Sensitivity of different 3D force sensor structures fabricated from SOI wafers.* α *and* γ *represent the angles in the spherical coordinate system: the angle in the x-y plane and the angle between the force vector and the x-y plane, respectively.*

BioMEMS and Microfluidics

Activity leader: P. Fürjes
Group members: Zs. Baji, I. Bársony, Cs. Dücső, Z. Fekete, Z. Hajnal, and A. L. Tóth

Activities are supported by:
- OTKA K108366 - Creating microchannels by Proton Beam Writing and their applications in Lab-on-a-chip devices (2013-2017)
- ENIAC_08-1-2011-0006 - Chip Architectures by Joint Associated Labs for European diagnostics CAJAL4EU (2010-2013)

Significant numbers of the environmental or clinical analytic tests are targeting the quantitative or qualitative analysis of different molecules in air or liquid samples. The micro and nanotechnology based sensing principles enable the development and realisation of robust, user-friendly and cost-effective analytic platforms.
Recently significant efforts were devoted to set up a competitive infrastructure and acquire solid background knowledge in the Microtechnology Laboratory of MFA for supporting the development of biosensors, bio-interfaces and microfluidic systems. The related scientific fields involved micro- and nanofluidics, bio-analytical and medical diagnostics (BioMEMS) research. As proven by the numerous ongoing projects and also by the growing interest of industrial partners, this emerging field is highly challenging. The research field is most attractive for Ph.D., graduate and undergraduate students as well. Our main goal is to develop integrated systems for industrial and medical applications, as demonstrated successfully in several projects in cooperation with industrial partners like Tateyama Kagaku Ind. Corp. Ltd. (Toyama, Japan), NORMA Diagnostics, (Wien, Austria), 77 Elektronika (Budapest, Hungary), Micronit (Twente, The Netherlands).

- Besides the development of conventional micromechanical sensors, a reliable background was established at MFA for the research and development of bioanalytical and medical diagnostic systems in form of a complex laboratory for characterisation of microfluidic and BioMEMS devices.
- The established system technology is capable to fabricate complex micro- and nanofluidic systems in silicon/glass and polymer materials.
- A wide cooperative network and knowledge base in the topic was set up by the research projects we participated in.
- The scientific and processing results are directly transferred into higher education, which is represented by the number of students working in the laboratory on their TDK, B.Sc., M.Sc. or Ph.D. theses.

Integrated bioanalitycal systems based on nanopore arrays
The application of complex nanofabricated structures is increasingly demanded in the field of mechanical, chemical and biochemical transducers. As a result, innovative biosensing principles, new capabilities for medical applications are offered. Chemically modified nanonopore based sensors, e.g. can be applied to detect specific biomolecules electrochemically via transport modulation by molecule binding in

pores. Nanopore sensing was envisioned to provide a new generation, nanoelectronics-based high sensitivity, label-free medical diagnostic platform. The main targeted application was the diagnosis of cardiovascular diseases (CVD) through relevant biomarkers (primarily cardiac Troponin I (cTnI).

Individual and fluidically integrated solid-state nanopore arrays

The nanopore based sensors proposed in the CAJAL4EU project were fabricated by the combination of silicon micromachining and nanofabrication processes, applying Focused (Ga^+) Ion Beam (FIB) milling of nanopores in a Silicon-Nitride membrane. Gold coated Silicon-Nitride layers provided mechanically stable membranes with controlled pore geometries for bio-functionalization. To establish a reliable fabrication process the FIB drilling was characterized and improved to achieve accurate pore geometry by computer controlled nanomachining. The nanopore membranes were integrated into an electrochemically addressable fluidic system

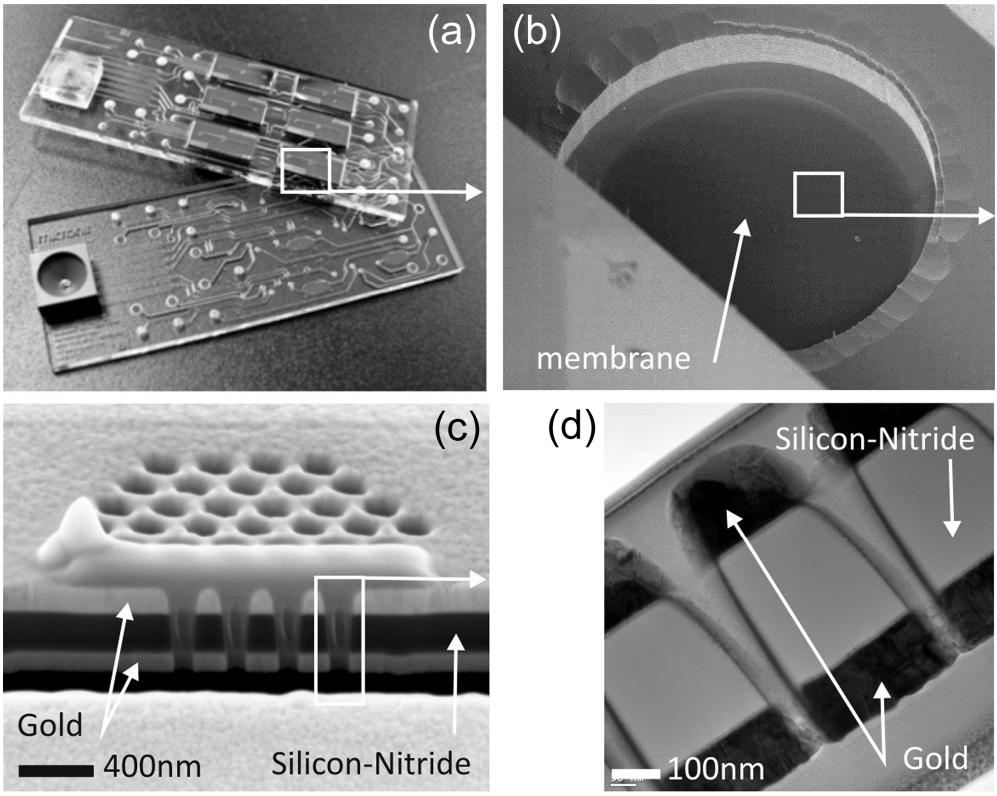

Figure 1. *(a): Biosensor cartridge with integrated fluidic and electrical addressing of six nanopore chips for multiplexed measurements, (b): Gold/Silicon-Nitride/Gold multilayer structure of the individual nanopore chips in which the nanopores are milled by FIB, (c): SEM image of the FIB nanopore array, (d): TEM image of the nanopore cross section.*

comprising the fluidic channels and electrodes. The 3D fluidic channel system of the individual nanopore chips was micromachined in Si/glass heterostructure and bonded to the multichannel fluidic cartridge, designed and fabricated by 77 Elektronika and Micronit, accommodates six nanopore chips for multiplexed measurements.

System integration and the development of the nanopore platform prototype
A prototype of the integrated nanopore platform was designed and constructed interfacing of the disposable biosensor cartridge through a custom holder to the electrochemical measurement and microfluidic actuation systems.

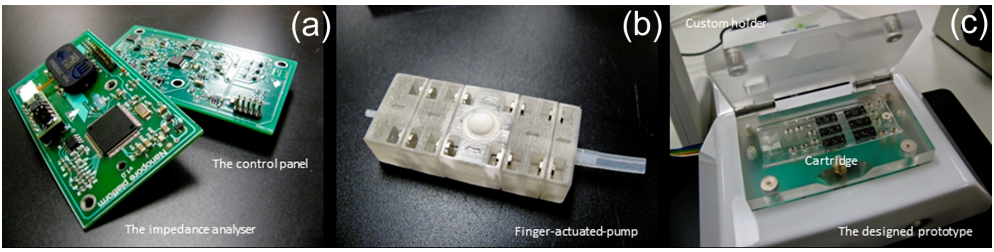

Figure 2. *Prototype of the nanopore platform: (a): impedance analyser, (b): finger-actuated micropump, (c): the complete system with the biosensor cartridge.*

The electrochemical read-out is facilitated by an AC electrochemical impedance analyzer - measuring nA currents in the range of 100kHz to 1Hz. The complete system is manufactured in a portable hand-held device format, which can be connected to any PC via micro-USB. The device control and the data evaluation are done through a user-friendly GUI. The prototype of the integrated nanopore platform is able to measure up to six independent markers sequentially just from a single sample. The required sample volume is 9µl from serum and 18µl from whole blood.

Biomarker detection with biofunctionalized nanopores
The high-throughput characterization of novel, extremely stabile, high affinity artificial bioreceptors (aptamers, spiegelmers) to comply with the specific requirements of nanopore sensing was developed by researchers of the Semmelweis University and the Budapest University of Technology and Economics. Receptors were characterized in terms of binding properties by using novel high throughput SPR imaging and optical bioassay methodologies. The spiegelmer receptor developed for cTnI enables the selective detection of cTnI in serum *without any additional reagents, which is a major breakthrough*. Extremely high sensitivities in serum samples were obtained for cTnI detection (LOD ca. 1 pg/ml) by nanopores. This is a *label-free troponin measurement method of unprecedented high sensitivity!*

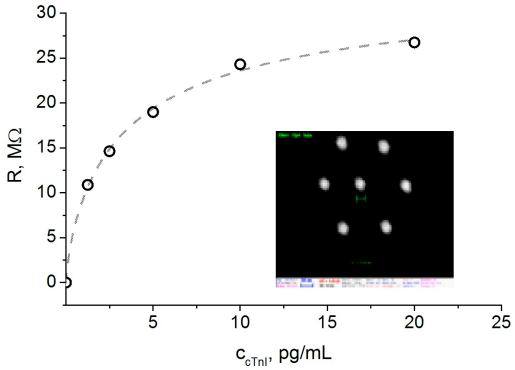

Figure 3. *Typical calibration curve of cTnI in the high sensitivity range measured with a nanopore array of seven 30 nm diameter pores (inset) sensitized by spiegelmer receptor.*

The nanopore platform team achieved a significant progress beyond state of the art in terms of: (i) nanopore fabrication by FIB, (ii) on-chip fluidic integration of nanopores, (iii) discovery and implementation of novel highly stable, selective and cost-effective receptors (spiegelmers, PNAs) as well as novel high throughput methods for their characterization, (iv) bio-functionalization of gold-coated and SiNx nanopores, (v) development of high sensitivity label-free nanoelectronic detection methodology, (vi) design and fabrication of the complete range of hardware and software for autonomous use of nanopore diagnostic platforms.
The feasibility of the nanopore platform for diagnostic measurements was demonstrated with the selected cTnI biomarker. Furthermore, essential know-how was gathered for establishing the bio-functionalized nanopore sensing as universal platform for a wide range of biomarkers.

Development and characterisation of functional passive microfluidic devices
The rapid development of microscale medical diagnostic devices has pointed out the importance of microfluidics enabling quick and effective transport, preparation and analysis of liquid biological samples. In microscale, otherwise trivial sample preparation methods, such as effective mixing of fluids as well as the size-dependent separation of corpuscles and their filtering from the blood might become a challenge. A low cost and comfortable sample loading and on-chip transport is thus also an important question in medical application.

Particle motion in microfluidic structures
Besides microscale characterisation of the hydrodynamic behaviour of conventional fluids, the analysis of the real biological samples, the investigation of special properties of the fluid (blood) and the physical properties of the particles (cells) is also a critical requirement.
Computational fluid dynamics (CFD) simulations, trajectory modelling and laboratory measurements were carried out to characterise in detail the performance of various microfluidic mixer structures utilising chaotic advection. The mixing performance of Herring-Bone type chaotic mixers constructed with various geometric parameters was studied by FEM modelling. The developing particle distribution in

the microfluidic structures with different geometries were visualized by Poincare-maps. The results of the simulations showed that for improved performance of the mixer we should increase the number or the width of the grooves in the Herring-Bone structure. The results of simulations were verified experimentally by recording the particle trajectories by dark field microscopy. The experienced behaviour was in good agreement with the results of the simulations. The modelled trajectories of the individual particles confirmed the experimentally observed main hydrodynamic effects, pressure gradients and shear forces.

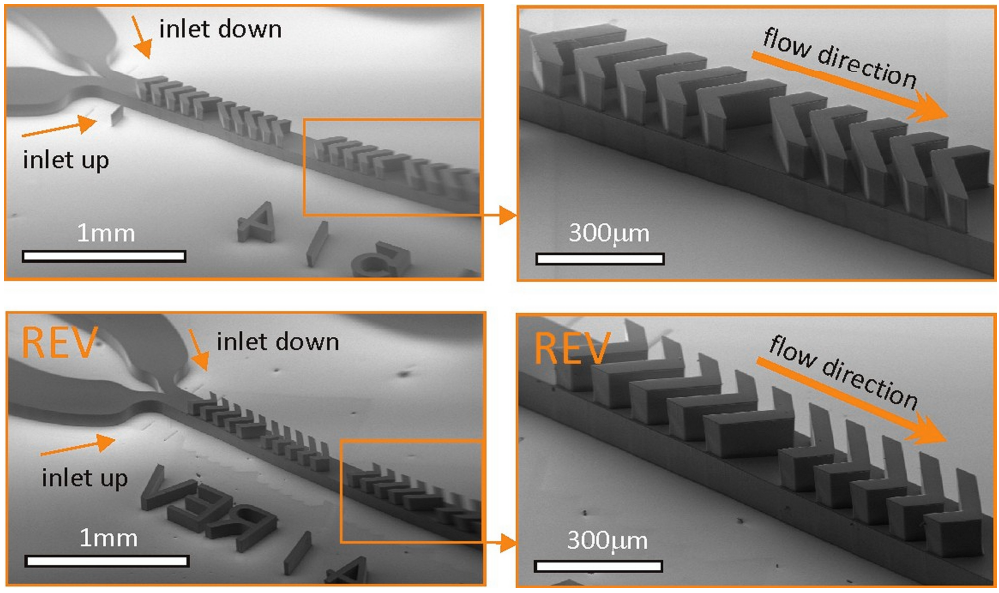

Figure 4. *Multilayer SU-8 molding masters of different Herring-bone mixer designs for PDMS structuring.*

The behaviour of real particles (blood cells) in special microfluidic structures was characterised by both numerical modelling and measurements for analysis of the size dependent separation, especially the physical phenomenon of lateral migration. Based on the simulation results test structures were fabricated by fast prototyping and the main characteristics of the selected structures were studied.

Surface modification of microfluidic structures

Surface modification methods were also studied to improve both wettability and non-specific protein binding of PDMS. Triton X-100 surfactant and PDMS-PEO were added to the raw PDMS before polymerization. The influence of embedded molecules was analysed in terms of contact angles and functionality. Contact angle of the modified PDMS surfaces was decreased by up to 30% and 50% by PDMS-PEO and TX-100 surfactant molecules, respectively. This reflects the changing of the surface of PDMS from hydrophobic to hydrophilic. Moreover, we found in both cases that irreversible protein adsorption on the PDMS surface can be decreased by almost 100%.

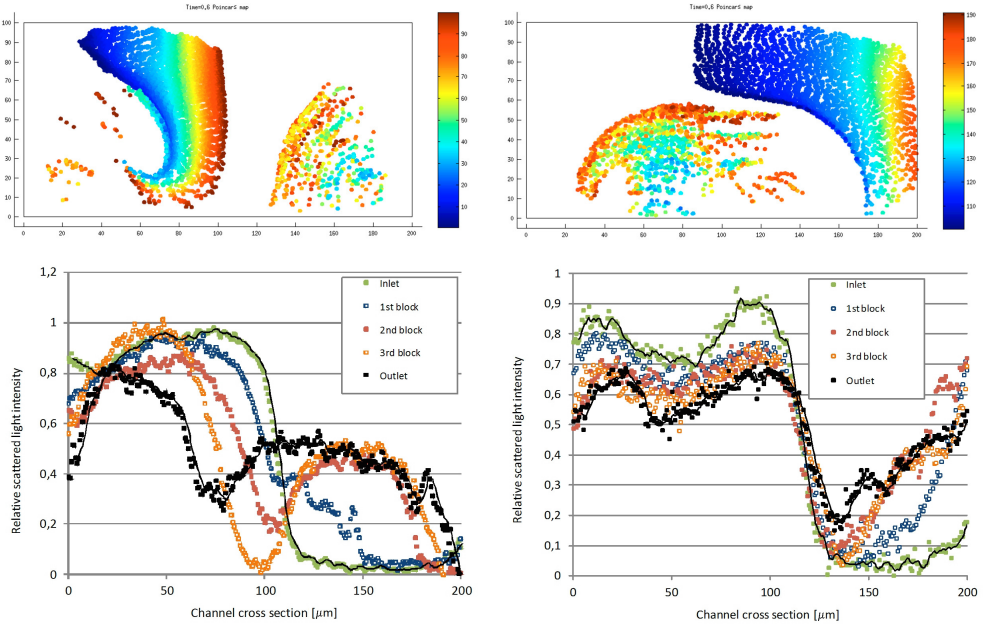

Figure 5. *The Poincare maps represent the particle mixing in the plane perpendicular to the channel direction and heading with the flow front in the Herring-Bone structure: forward–left/reverse-right (top images). The relative light intensity scattered from the fungi cells reflects the particle distribution in the cross section of the Herring-Bone mixer structure in different cross-sectional planes (bottom images).*

Mechanical biosensors for particle and molecule detection

Microcantilever structures were designed and fabricated by the application of recently developed surface micromachining process. The microfabricated test structures were characterised for mechanical stability, deformation, resonance frequency. Investigations definitely require the controlled actuation of the microstructures as well as a precise detection of deformation when applying optical, piezoelectric or piezoresistive read-out.

Electromagnetic model of cellular flow in a microfluidic system

Impedance based flow cytometry is a well-known cell-counting and characterising method in and wide spread use. Flow cytometry is powerful in counting, sorting or differentiating cells, or larger particles which have diverse characteristic physical properties. The electromagnetic field evolving in the sample fluid was characterised when particles are travelling in a microfluidic system containing platinum electrodes deposited on the borosilicate glass surface of the fluidic channel formed in crystalline silicon.

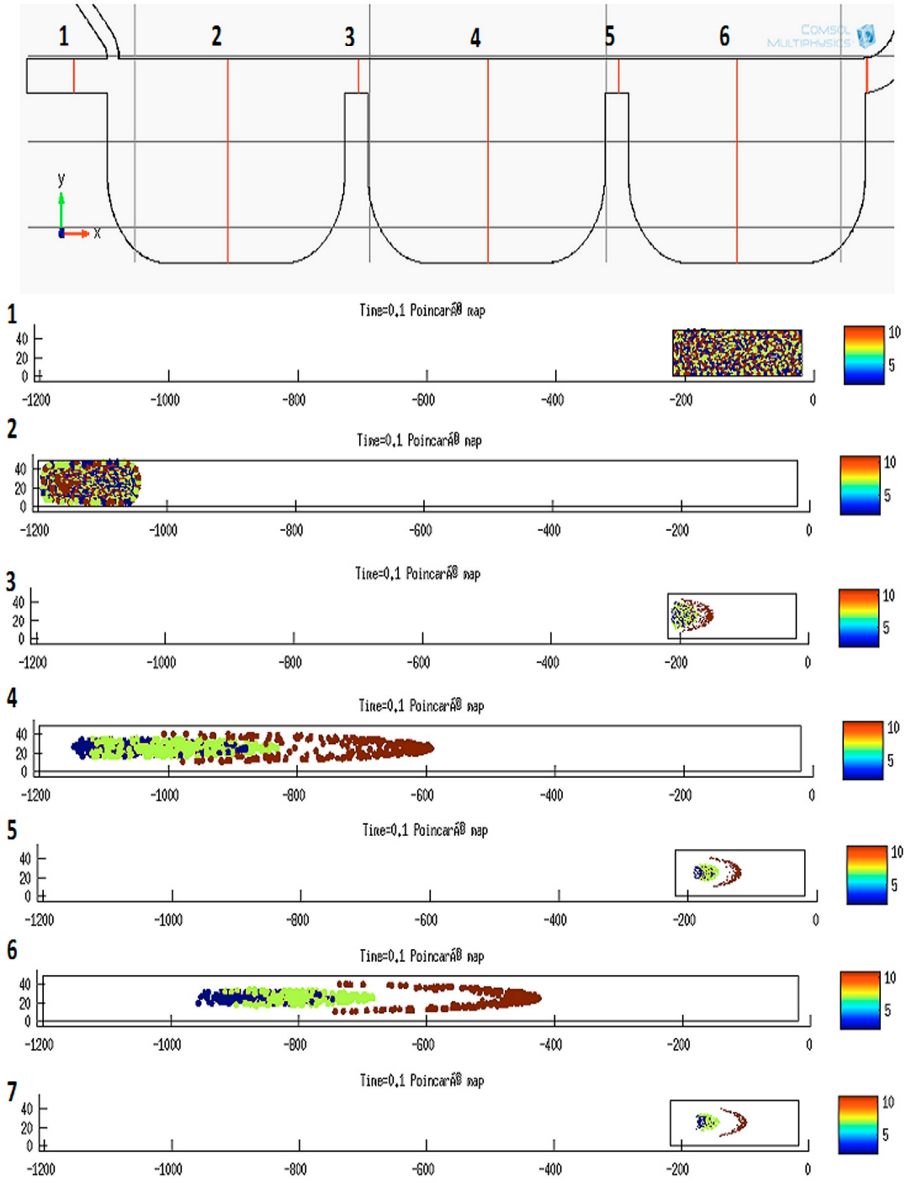

Figure 6. *Size dependent particle separation due to the lateral migration effect was modelled by FEM simulation. The particle distributions (d= 2 (blue), 7 (green) and 15µm (red)) are plotted in different cuts perpendicular to the microchannel.*

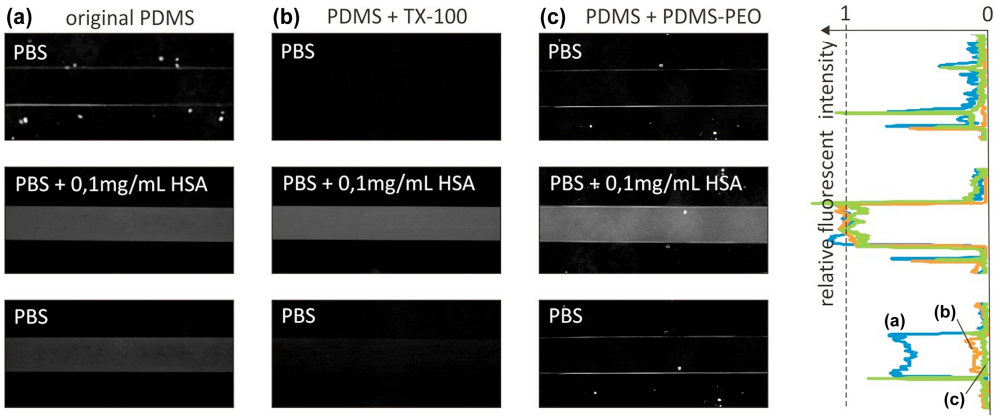

Figure 7. *Fluorescence intensity change in the microchannel recorded after FITC labelled HSA solution (0.1mg/mL HSA in PBS) was injected and washed by PBS. Decreased protein absorption was achieved when the original PDMS surface (a) was modified by 0.2v/v% TX-100 (b), and by 0.2%v/v PDMS-PEO additives(c).*

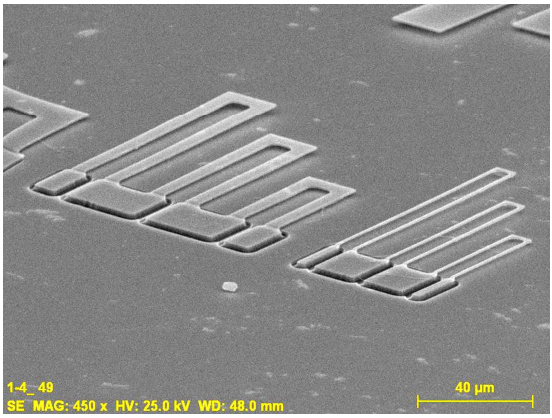

Figure 8. *Polysilicon microcantilever array prepared by surface micromachining.*

2D and 3D simulations were implemented by Matlab and Comsol Multiphysics, respectively, applying simple Dirichlet-boundary for the electrodes and Neumann-boundaries on the channel walls defined as non-conducting elements. The impedance characteristics were computed as the single red blood cell travelled along the channel in physiologic saline water between the electrodes vs. different geometry parameters as channel width, electrode lengths, electrode distance from each other, or the distance of the biological cell from the electrodes. DC and AC impedance and lifting force acting on the biological cell were also computed.

We could conclude that for efficient cell detection and differentiation we should apply low input voltage. The cells have to be positioned by hydrodynamic focusing close to the electrodes being on the same side of the channel (till cell lysis occurs), however, if the electrodes are on the opposite sides, focusing should be in the middle region. Moreover, the channel height and the width of the electrodes should be decreased (just until danger of clogging occurs). The results were applied for optimization of the further geometric design of detector chips including microfluidic channels and platinum electrodes, too.

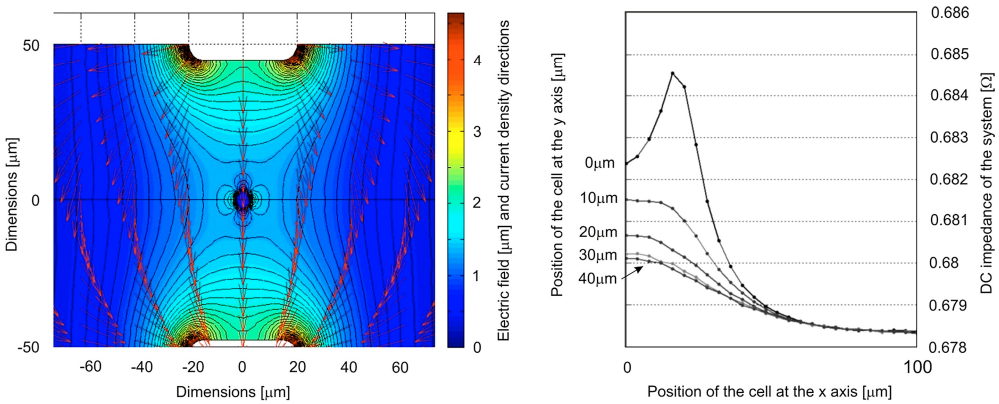

Figure 9. *Simulated electric field and current density evolving in a microfluidic channel (left) and DC impedance of the system as a function of the cell position (right).*

NeuroMEMS

Activity leader: Z. Fekete
Group members: P. Fürjes, Z. Hajnal, Gy. Molnár, A. Pongrácz, A. L. Tóth, Z. Bérczes, and G. Márton,

Activities are supported by:
- Targeted research activity supported by Gedeon Richter Plc.

Single-shaft microelectrodes combined with microdrives

Exploring neural activity behind synchronization and time locking in brain circuits is one of the most important tasks in neuroscience. These questions are intensively studied by using multiple electrodes to measure activity concurrently in different brain areas. A robust silicon-based microelectrode array with anatomically designed site arrangement was designed in order to record neural activity of freely moving rats in several brainstem nuclei, concurrently. A microdrive allows precise electrode positioning (and free repositioning) during chronic experiments. When the recording of single-unit activities is crucial, this ability is extremely useful.

In our system, the probe is fixed on a PTFE block of the micropositioner. The self-lubricating PTFE block travels smoothly on two tightly fit rods, its position can be adjusted with a driving screw (300 μm/turn). A flexible cable connection of 50 μm thick polyimide provides sufficient freedom for the movements of the drive. The robust structure of the device allows very stable probe location, and excludes vibration.

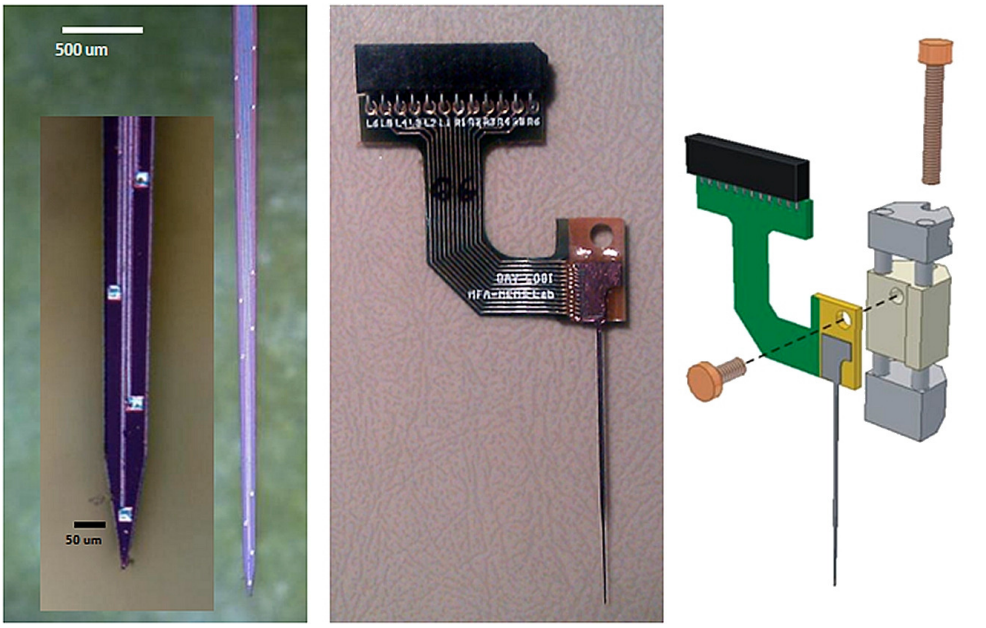

Figure 1. *Si microelectrode - microdrive system with flexible encapsulation.*

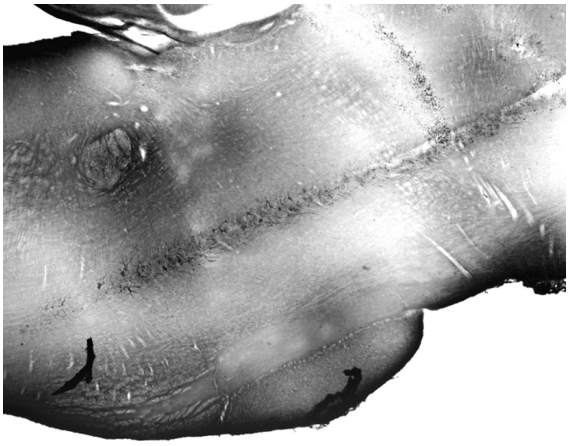

Figure 2. *Simultaneous long-term recording (up to 6 months) of single unit activity from three target areas.*

	Putative principal-like cells	**Local inter-neurons**
DpMe	23	8
PPtg	8	0
PnO	55 (37+18)	24
	86 (~73%)	32 (~27%)
	135 after sorting →**118**	

Figure 3. *Distribution of action potentials recorded in the target areas.*

Neural microelectrodes with local drug delivery and simultaneous electrical recording functions

The fabrication method, electrical and fluidic characterization and in vivo testing of the first silicon deep brain multielectrodes (up to 70mm long) with monolithically integrated fluidic channel were studied. Both the electrical and fluidic performance of the probe was investigated. Field potential, multi- and single unit activities were recorded. Measured and calculated hydrodynamic resistance of the microchannels showed good consistency. The typical volumetric flow rate values are in the 0.5–5 µl/min range at pressures below 200 kPa. The performed in vivo test proved that the fabricated hollow microprobes are applicable as stable drug delivery devices in neural implants. Simultaneous electrical recording is provided even in deep brain regions. This technology is robust and scalable. Custom made drug outlets and recording/stimulating sites can be integrated in order to fulfil requirements of special experiments. The proposed technology still preserves the freedom of further integration of microcomponents, e.g. fluidic actuators, micromixers, optical waveguides and biosensors, opening the door to more complex and delicate investigation of the central nervous system.

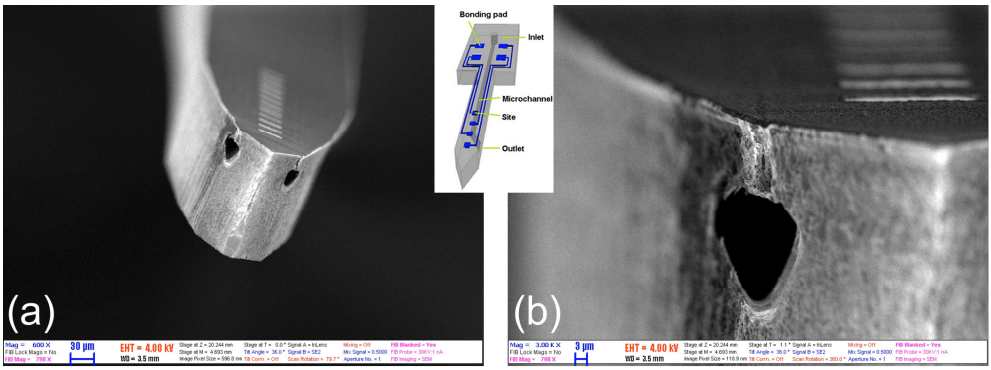

Figure 4. *Micrograph of the first silicon deep brain multielectrode with monolithically integrated fluidic channel (a), and close-up SEM view of the fluidic outlet of a buried microchannel (b).*

Surface enhancement of silicon microelectrode array by black-platinum

Despite the broad spectrum of already published methods, impedance reduction of electrodes of neural microelectrode arrays (MEAs) is still an issue under active research. A key factor to be considered is whether these deposits are durable enough to withstand the penetration into the neural tissue. The durability of high surface area platinum electrodes during acute intracerebral measurements was investigated. Electrode sites with extremely rough surfaces were prepared by electrochemical deposition of platinum onto silicon-based MEAs from a lead-free platinizing solution. The close to 1000-fold increase in effective surface area lowered the impedance, its absolute value at 1 kHz dropped to about 7% and 18% of the original Pt electrodes in vitro and in vivo, respectively. 24-channel probes were subjected to 12 recording sessions, during which they were implanted into the cerebrum of rats.

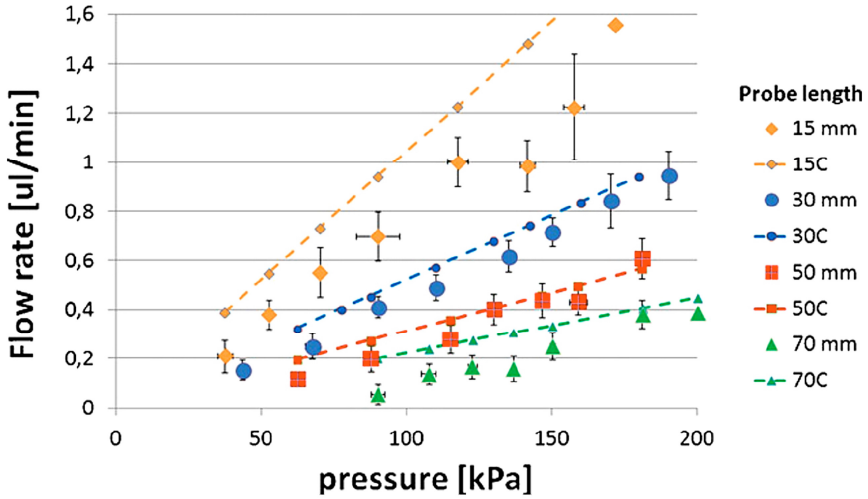

Figure 5. *Measured and calculated flow rate vs. pressure characteristics of a hollow microprobe for different probe lengths.*

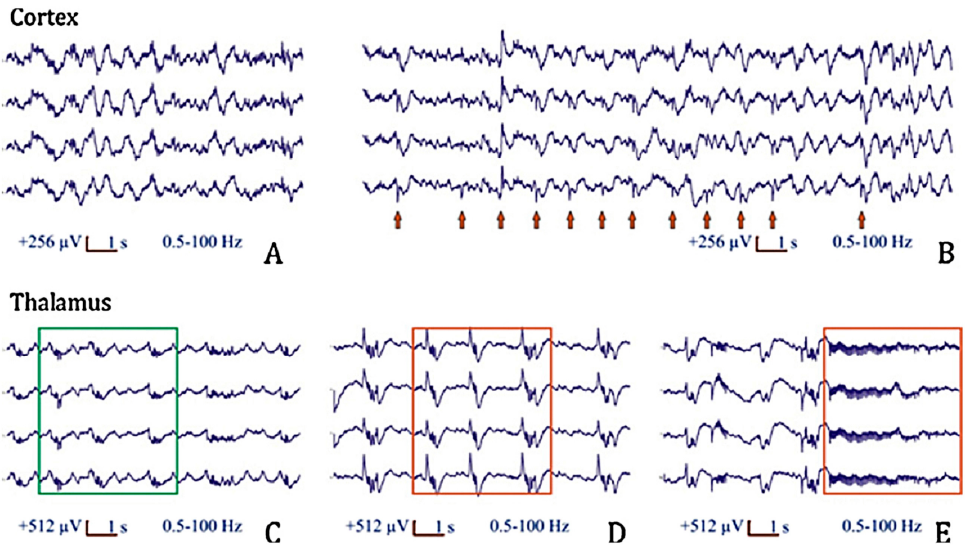

Figure 6*. Local field potential signals in rat cortex, band-pass filtered at 0.5–100 Hz, showing slow wave activity before injection (A). Bicuculline caused elevated neural activity, which is indicated by interictal-like spikes on the local field potential signals. These local field potential spikes are marked by red arrows (B). In the thalamus, signals were recorded during normal activity (C), and under bicuculline-induced conditions, such as interictal-like spikes (D), and high-frequency epileptic-like events (E).*

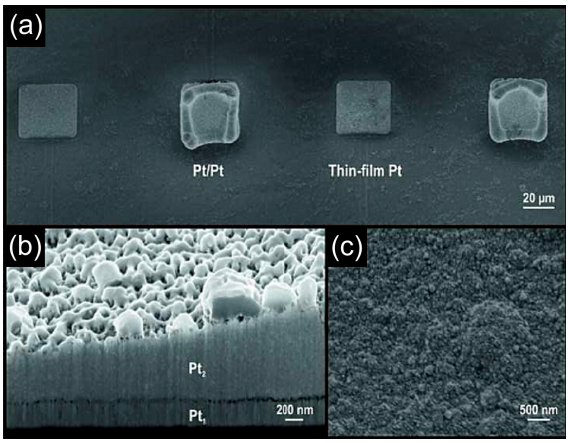

Figure 7. *(a): Scanning electron microscopic images of four neighbouring electrode sites on the MEA, two of them coated with Pt/Pt, (b): A cross-sectional view of the Pt/Pt layer, sectioned by Focused Ion Beam (FIB). Pt1 is the original thin-film, Pt2 is the electrochemically deposited layer. (c): Surface microgram of deposited platinum (Pt/Pt electrode).*

Although the effective surface area of the platinized sites mostly decreased, it remained more than two orders of magnitude higher than the average effective surface area of the sputtered original platinum thin-film electrodes. Sites with electrochemical deposits proved to be superior, e.g. they provided less thermal and 50 Hz noise, even after 12 penetrations into the intact rat brain.

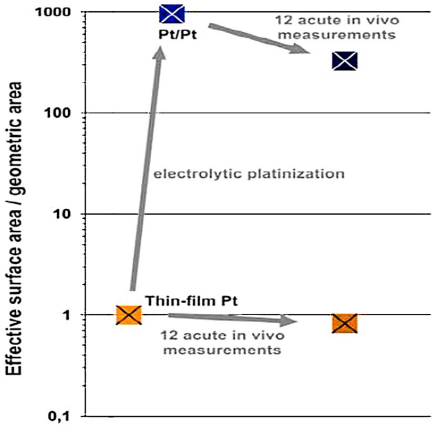

Figure 8. *The variation of average effective surface area with electrolytic platinum deposition and multiple acute use of the MEAs.*

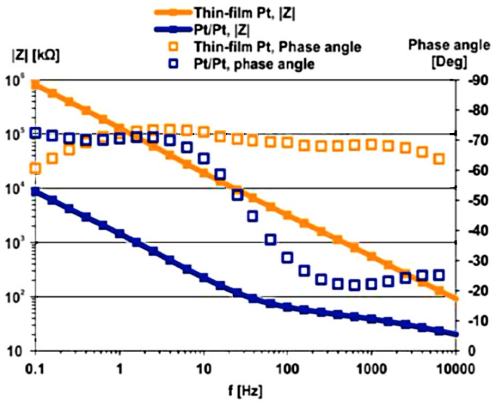

Figure 9. *Average EIS spectra of original thin-film Pt and Pt/Pt electrodes on a probe.*

Mechanical interaction between single-shaft silicon microelectrodes and rat dura-matter

Due to the rapid development in micro- and nanofabrication technologies, several types of medical implants were proposed and applied successfully in neurosurgery. In order to determine the safety margins and design rules for newly emerging techniques, in vivo mechanical characterisation is essential to be performed. In our

work, experimental investigation is presented focusing on the interaction between rat brain tissue and single-shaft silicon microprobes fabricated by deep reactive ion etching. Physical parameters like penetration force and dimpling were studied in terms of insertion speed (mm/min range) and microprobe cross-section. Insertions were performed through intact *dura* and *pia* matter.

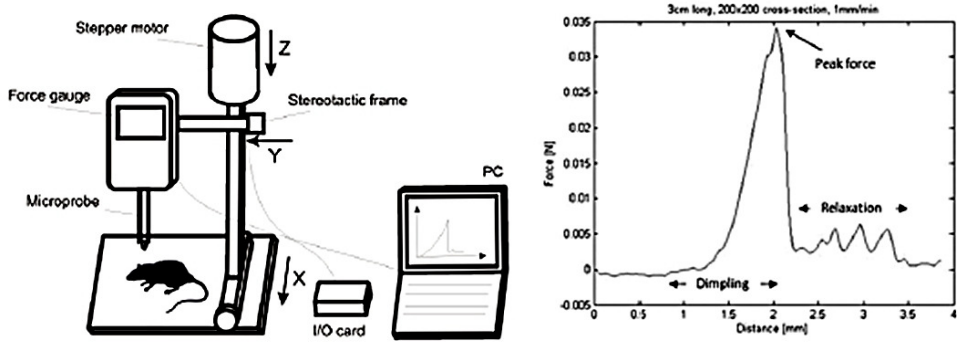

Figure 10. *Schematic representation of the experimental setup for in vivo testing of penetration mechanics (left) and a typical force vs. distance curve (rights).*

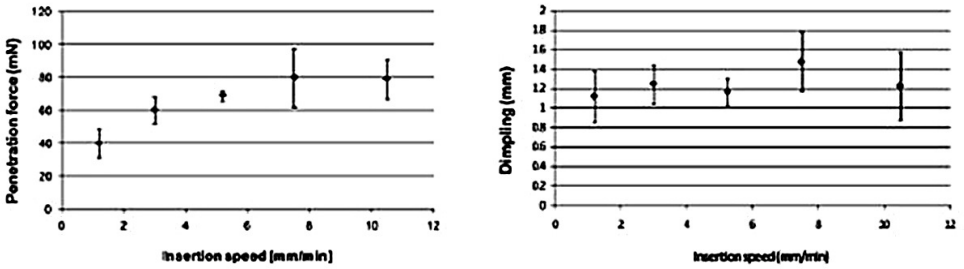

Figure 11. *Measured penetration force and dimpling at various insertion speed with a probe cross-section of 200 × 200 μm^2.*

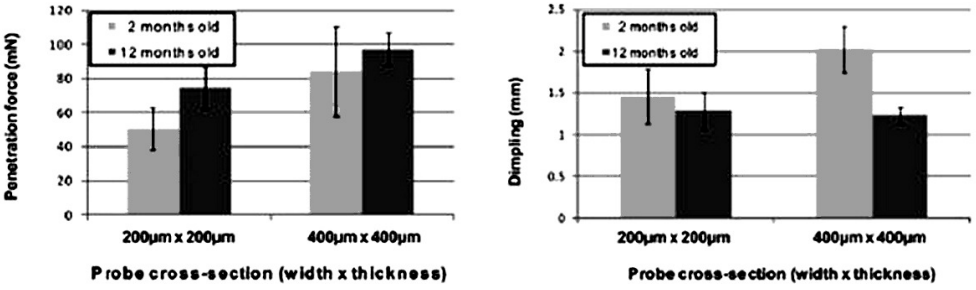

Figure 12. *Measured penetration force and dimpling as a function of rodent age in case of two different probe-cross-sections.*

Polymer-based microelectrode arrays for electrophysiology

Polymers attract increasing attention as bulk materials for microelectrode arrays, applied in experimental electrophysiology and clinical use. Their fabrication costs are relatively low, and their flexibility allows smoother coupling with the soft neural tissue than do rigid substrates. Sufficient biocompatibility of the applied materials is essential in this field. Several types of polymers, such as SU-8 photoresist, Polyimide (PI) and Parylene C meet this criterion. Polymer-based device components for neural interfacing show great heterogeneity in structure and function. In order to obtain electrical connection with the central nervous system, cerebral implants are available. Interfaces with peripheral nerves can be constructed with sieve, cuff and transverse probes. Microfabricated polymer structures are commonly applied for electrocorticography (ECoG) as well, which is a widely used method for the localization of epileptogenic zones. At the Department of Microtechnology, we have developed various microtechnology related processes which are required to create – among others – such structures. We use silicon wafers as substrates. The key components of the process flows are SU-8 lithography, patterning metal layers with lift-off technology and reactive ion etching of polyimide. Utilizing these methods, e.g. PI – Pt – SU-8 three-layer structures can be formed. We constructed various, custom-designed, polymer-based probes for both in vitro and in vivo electrophysiological applications.

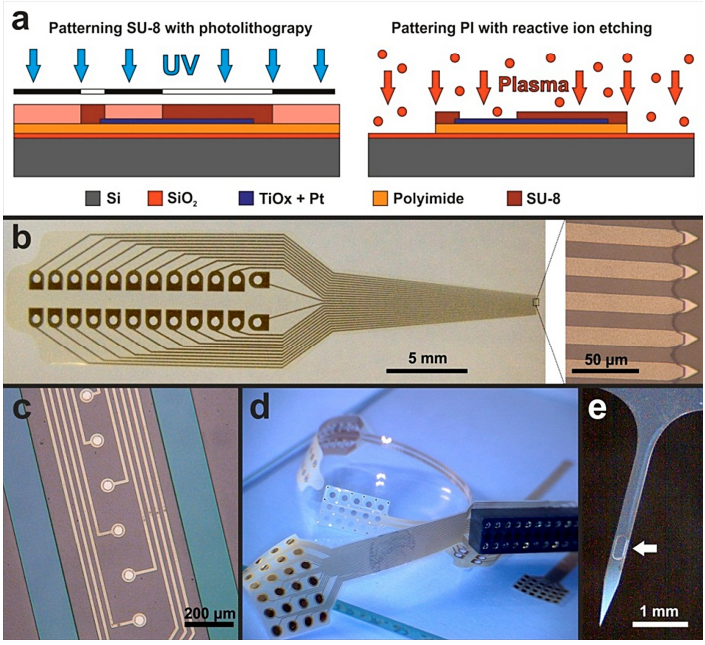

Figure 13. *(a): patterning of SU-8 and polyimide layers in microfabrication. (b): examples of polymer-based neural probes manufactured by our group: a "spiky" electrode array for in vitro analysis of brain wafers. (c): an intracerebrally implantable extracellular array. (d): electrodes designed for electrocorticography. (e): a probe with a microwell, which can contain e.g. bioactive molecules.*

NEMS

Activity leader: J. Volk
Group members: Zs. Baji, G. Battistig, Cs. Dücső, P. Földesy, N. Q. Khánh, I. Lukács, Gy. Molnár, A. L. Tóth, Zs. Zolnai, R. Erdélyi Z. Szabó, and I. Bársony

Activities are supported by:
- OTKA K109674 – Graphene-based terahertz modulators (2013-2017)
– EU FP7-ICT-2013-10- 611019 - High-resolution fingerprint sensing with vertical piezoelectric nanowire matrices (PiezoMAT) (2013-1015)

Investigation of quasi-one-dimensional compound semiconductor nanostructures
The semiconductor nanodevice activity focussed on the synthesis and characterization of quasi-one-dimensional semiconducting nanostrucrures, as well as on their integration into functional sensor, optoelectronic and photovoltaic devices. The explored research fields include the electrical characterization of hydrothermally grown high aspect ratio ZnO nanowires, the mechanical characterization of vertical nanorods, the synthesis and characterization of hierarchical ZnO nanostructures, as well as a new research topic related to TiO_2 atomic wires.

Characterization of Field Effect Transistor Based on Hydrothermally Grown ZnO Nanowire
Since the last decade zinc oxide nanowires (ZnO NW) became potential candidates in sensor applications. The transducer in most cases of chemical and biosensors is a ZnO NW based Field Effect Transistor (FET). In such application for obtaining an acceptable noise/signal ratio it is important to fabricate good contacts to the NW. The other essential point is its gating behaviour, which determines the sensitivity of the sensor. We have prepared the FETs based on hydrothermally synthesized ZnO NW, and characterized them observing the above aspects electrically.
Synthesis of ZnO NWs was carried out from Zn foil in solution of sodium hydroxide and ammonium persulfate (W1), or from sputtered ZnO seed in aqueous solution of zinc nitrate/ hexamethylenetetramine (W2). In some cases the NWs were annealed at 200 or 600 °C in air for 30 min. Contact formation of the NWs with Al or Ti/Au was realized by using e-beam lithography, metal deposition and lift-off.

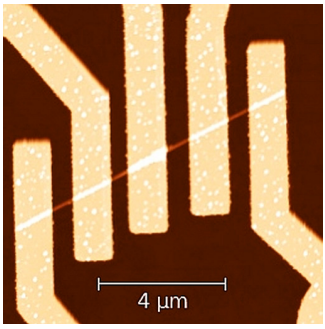

The AFM image of a NW having multiple contacts is presented here. By means of I-V measurement on each contact pair, one can determine the contact and wire resistance (Transfer Length Method), respectively, as depicted on the right side of the figure. These parameters can also be obtained by four-wire measurement, where the voltage drop between the inner contact pair was measured while forcing a constant current through the outer contacts.

Figure 1. *AFM image of contacted ZnO NW.*

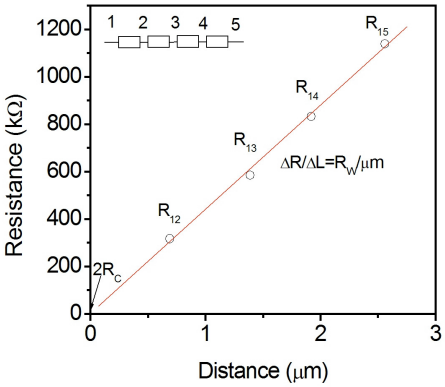

Figure 2. *TLM measurement of Ti contacted ZnO NW.*

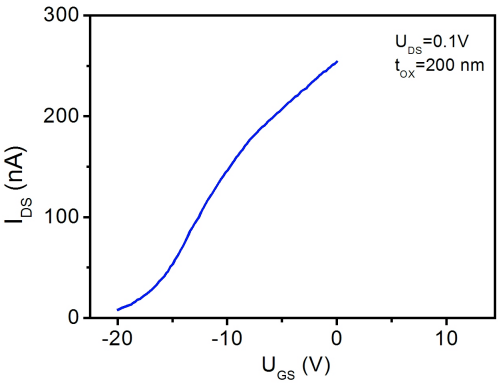

Figure 3. *I_{DS}-V_{GS} characteristics of Ti contacted ZnO NW.*

Using degenerately doped Si substrate as global back gate, the I_{DS} vs. V_{GS} function can be recorded, from which one can deduce the values of transconductance (g_m), surface mobility (μ), carrier concentration (n_i), and threshold voltage (V_{th}).
The results are summarized in the table below. The non-annealed W1 wire is rather metallic, presumably due to high charge carrier concentration in the NWs, which causes low contact resistance, but makes the gating impossible. The gating effect is significant only for the W1 NW annealed at 600 °C, probably due to the out-diffusion of hydrogen incorporated into ZnO during the synthesis process. The W2 NWs are superior to W1 ones, because they can be gated without post annealing. Furthermore, their typical thickness is less than that of the W1 NW's, which enhances the sensitivity of the NW-based sensor via a complete depletion of the conducting channel.

Table I. *Parameters of ZnO NW based FETs*

Samp./T_a/Contact	Spec. R_c (x10^{-7} Ωcm^2)	Spec. R_w (mΩcm)	V_{th} (V)	g_m (nS)	μ (cm^2/Vs)	Carrier conc. (x10^{18} cm^{-3})
W1 RT Ti	2.5	3	-	-	-	-
W1 RT Al	3.0	3	-	-	-	-
W1 200 °C Al	4.4	2.6	-	-	-	-
W1 600 °C Ti	110	130	-17.8	20	17.6	4.0
W1 600 °C Al	72	113	-13.1	98	22.7	6.7
W2 RT Ti	340	40	-	-	-	-
W2 RT Al	326	10	-11.8	34	52.4	14

Bending strength analysis of vertical ZnO nanowires

For the practical applications of vertical nanowires in Nano-ElectroMechanical Systems (NEMS) it is pivotal to maintain mechanical strength, since they are often exposed to heavy duty use during operation. Aqueous chemical method is widely used for the growth of ZnO nanostructures, since various morphologies in a predefined fashion can fairly easily be achieved. However, 'as prepared' wet

chemically grown NWs show poor mechanical behaviour compared to their counterparts synthesized by physical methods at higher temperatures.
To overcome this latter problem, while retaining the benefits of aqueous chemical growth, we applied different heat treatments right after the synthesis in order to improve the mechanical properties. The effect of annealing temperature and annealing atmosphere was studied by our *in-situ* static bending setup inside the SEM. The arrangement is composed of a nanomanipulator robotic arm equipped with a calibrated AFM probe, which was used to bend the NWs at their free end until fracture occurred. The maximal strain generated at the root of the NWs right before the fracture was estimated by analysis of the videos captured during the manipulation. The most significant improvement in the robustness was achieved by applying an annealing temperature of 700 °C for 2 hours in oxygen atmosphere. Hence the maximal strain increased from 1.2 % to 3.8 % and the magnitude of the load needed to fracture the NWs became almost half an order of magnitude larger.

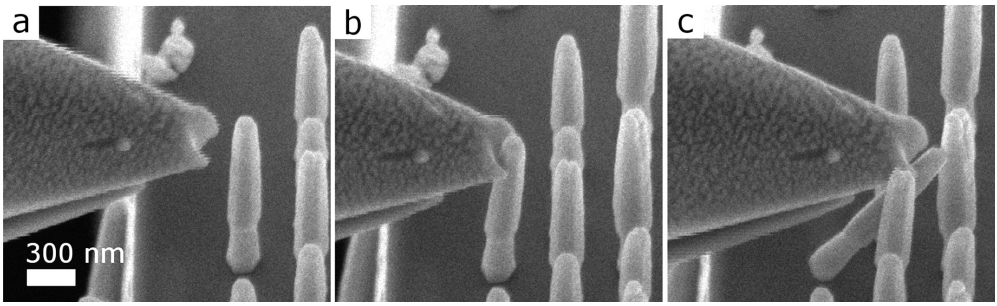

Figure 4. *Scanning electron micrographs showing the steps leading to the fracture of a ZnO nanowire of poor mechanical properties: positioning the tip(U-shaped) of the AFM probe close to the nanowire before manipulation (a), bending of the nanowire by the lateral load at its free tip (b), and fracture at its root (c).*

Another quantitative way of the mechanical characterisation of vertical nanowires can be done by atomic force microscopy (AFM), since during scanning both cantilever deflections and torsions are monitored by a position-sensitive photodetector. The obtained normal and lateral force signals can provide information about normal and lateral forces acting on the tip. However, in the normally used indirect calibration methods many error sources exist. To apply a known lateral force on the AFM probe we used a sheet of pyrolytic graphite which is levitated by a strong magnetic field, as a reference spring. Due to the direct nature of this detection method, the applied loads and hence the elastic moduli of nanostructures can be determined with high confidence, without the need for detailed information (e.g. geometry, resonant frequency) of the cantilever. The proposed technique was successfully applied for the quantitative characterization of NW fractures.

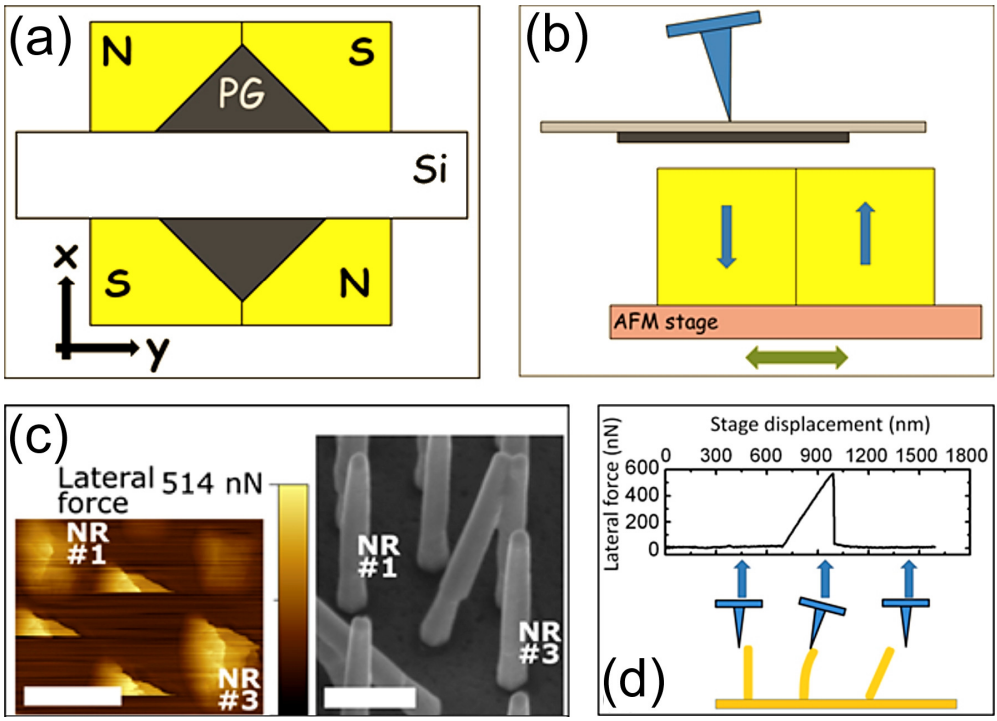

Figure 5. *Scheme of the D-LFC method: (a): the pyrolytic graphite sheet - Si wafer assembly is levitated by a strong magnetic field (top-view), (b): the diamagnetic levitation spring system mounted on the AFM stage to calibrate the lateral PSPD output, (c): typical lateral force map recorded during fracture events with the corresponding SEM image, and (d): the recorded bending curve.*

Investigation of hierarchical ZnO nanostructures for dye-sensitized solar cells

Dye-sensitized solar cells (DSSCs) are attracting considerable attention, as they may offer a promising alternative for silicon-based solar cells. This is because of their reasonably high power generation efficiency that comes at a low cost without environmental risks. The most efficient DSSCs apply TiO_2 nanoparticles. ZnO, however, is also often considered as a good candidate, too, since its more than one order of magnitude higher bulk electron mobility. Moreover, there is a great variety of fabrication techniques available for micro- and nanostructured ZnO.

In order to maximize the specific surface and thereby the dye uptake of the nanostructure, a novel synthesis route was demonstrated for the preparation of hierarchical ZnO structures. The fabrication technique combines a self-assembled nanosphere photolithography technique with multiple steps of low temperature hydrothermal ZnO growth.

The investigated nanostructure geometries include as grown random ZnO nanowires (NW), short and long regular pillars (SP, LP), short pillars covered by a porous ZnO layer (SP+PL) and long pillars with shorter or longer side branches (LP+short-SB, LP+long-SB), as well as ZnO thin film (TF) for reference. The specific surface area

was deduced from the absorbance spectra of the dye solutions after selective etching of ZnO nanostructure in NaOH water-ethanol solution. Assuming a uniform monomolecular coverage on the surface, effective roughness factors up to 10^6 were achieved. Some selected nanostructures were also used to fabricate solid electrolyte DSSC cell. The photoelectric characterizations revealed that the higher specific surface results in an enhanced short circuit current but too long side-braches can lead to smaller fill-factor and open-circuit voltage.

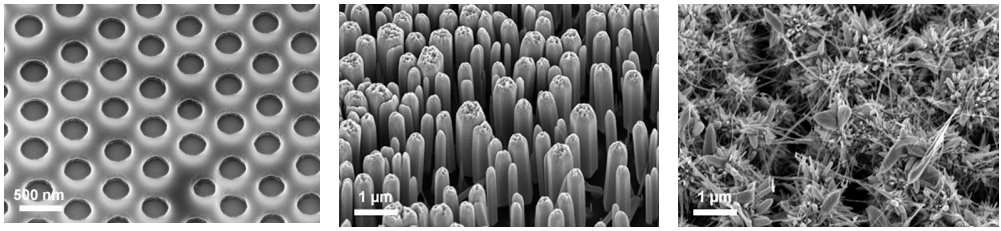

Figure 6. *(a): SEM images of developed photoresist, (b): hydrothermally grown ZnO pillars, and (c): ZnO pillars with hydrothermally grown side branches.*

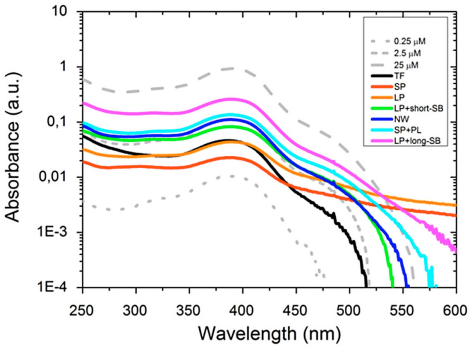

Figure 7. *Absorbance spectra of the calibration series (grey dashed lines) and the resolved dye solutions (colour lines).*

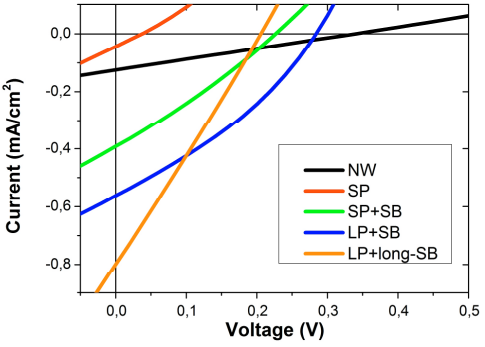

Figure 8. *Current-voltage curve of photovoltaic cells built with different nanostructure geometries.*

Structural Characterization and Contact Formation on Ultra-thin Anatase TiO_2 Nanowires

Wide band gap semiconductor titanium dioxide (TiO_2) is known as a versatile material with a wide range of applications. Nanostructures of TiO_2 in various crystal modifications are used among others in photocatalytic and photovoltaic applications. Recently, a new concept based on Dirac-states inside the conduction band of ultra-thin, n-type anatase TiO_2 nanowire (NW) was proposed to prepare high speed and good on-off ratio field effect transistors. To this end, we have characterized the structure of the TiO_2 NWs grown by non-hydrolytic solution approach. Then we successfully prepared contacts to such NWs, as first step to prove the above concept.

Structural characterization

The TiO_2 NWs first have been analysed by Transmission Electron Microscopy (TEM). The length of the wires was found to vary in the range of 10–40 nm, while their thickness is estimated to be around 3-3.5 nm. The picture shows the high resolution image (HRTEM) of the individual TiO_2 NW. The lattice fringes of the single crystalline NW are well resolved. The wire diameter is not uniform, but fluctuates about 25% along the longitudinal axis. The phase analysis using electron diffraction reveals that the crystal structure of our TiO_2 NWs is not rutile, but anatase, which was confirmed by X-ray diffraction analysis.

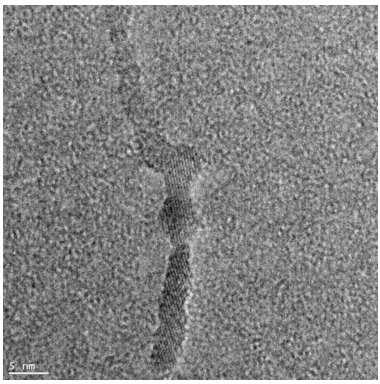

Figure 9. *High resolution TEM image of TiO_2 NW.*

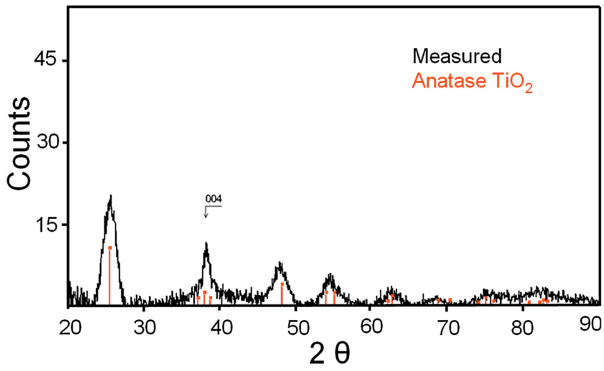

Figure 10. *XRD of the TiO_2 NW. (The pattern of anatase TiO_2 is also shown (red).)*

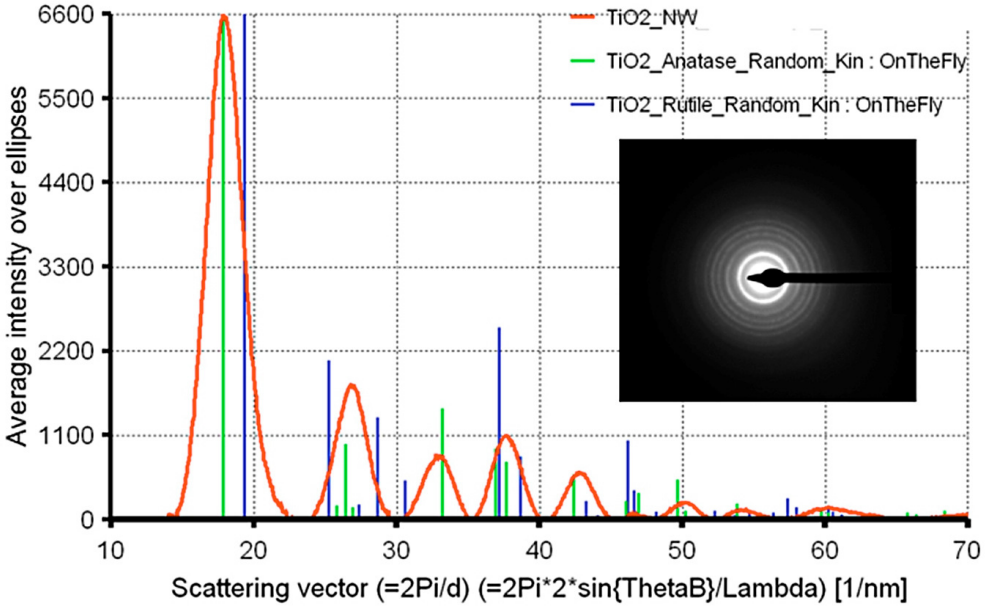

Figure 11. *Phase analysis of electron diffraction.*

Contact preparation

The TiO_2 NWs surface-stabilized by oleic acid was dispersed in cyclohexane, and deposited on top of the 100 nm thermal silicon-dioxide coated chip. The lithography of the PMMA e-resist layer was used for the formation of a pair of contacts with a gap of ca. 25 nm in two steps. The first one was the usual e-beam lithography to form a PMMA stripe with the width of 100 nm, which is the resolution limit of our system. In the second step oxygen plasma was applied to adjust the desired width by an optimized treatment time. This dry etch is gentle enough to prevent the collapse of final, very thin PMMA stripe, which could occur due to capillary force in the case of normal use of developer. The figure shows the AFM image of the TiO_2 NW contacted with 5 nm thick Cr layer. The thickness of the NW measured by AFM is about 3 nm, as confirmed by the TEM.

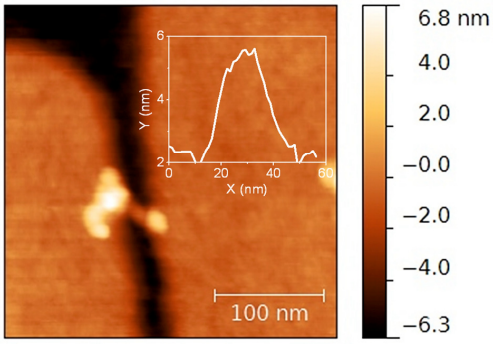

Figure 12. *AFM image of TiO_2 NW contacted by 5 nm thick Cr layer. The line-cut across the nanowire is shown in the inset.*

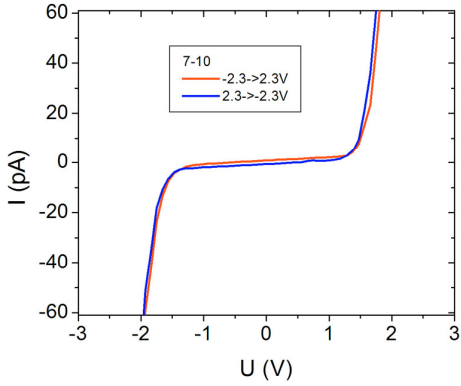

Figure 13. *I-V characteristics of Cr contacted TiO_2 NW.*

Preliminary I-V characterization was carried out on the Cr contacted NW. The device shows back-to-back Schottky behaviour, presumably due to the fact that the work function of Cr (4.5 eV) is higher than the electron affinity of TiO_2 (4.2 eV), thus forming a Schottky-junction at both Cr/TiO_2 interfaces.